Applied Physics Letters

RESEARCH ARTICLE | MAY 23 2013

# The "Shim-a-ring" magnet: Configurable static magnetic fields using a ring magnet with a concentric ferromagnetic shim

P. Nath; C. K. Chandrana; D. Dunkerley; J. A. Neal; D. Platts



*Appl. Phys. Lett.* 102, 202409 (2013)
https://doi.org/10.1063/1.4807778

# The "Shim-a-ring" magnet: Configurable static magnetic fields using a ring magnet with a concentric ferromagnetic shim

P. Nath,[a),b)] C. K. Chandrana,[a)] D. Dunkerley, J. A. Neal, and D. Platts
*Applied Modern Physics, P-21, Los Alamos National Laboratory, Los Alamos, New Mexico 87545, USA*

(Received 11 February 2013; accepted 2 May 2013; published online 23 May 2013)

We introduce a permanent magnet assembly that can be configured to obtain uniform, gradient, or tunable field distribution. The design is composed of a single ring shaped permanent magnet and a concentric ferromagnetic shim. Magnetic field is configured by changing the shape of the air gap inside the ring magnet. Circular cross-section produces up to 0.54 T uniform field, whereas rectangular or triangular cross-sections result in gradient magnetic field distributions. Tunable field from a given ring magnet is obtained by changing the thickness of the ferromagnetic shim or the spacing between the shim and the permanent magnet. © *2013 AIP Publishing LLC*. [http://dx.doi.org/10.1063/1.4807778]

Permanent magnets provide unique options for a wide range of applications including NMR (Nuclear Magnetic Resonance) spectroscopy, MRI (Magnetic Resonance Imaging), magnetic refrigeration, magnetic separation, motors/generators, and charged particle manipulations.[1] Depending on the type of application, the magnetic field desired from a permanent magnet requires precise design considerations. For example, a uniform field is required to perform NMR, whereas a gradient field is desirable for the manipulation of magnetic materials. Furthermore, there is also interest in tunable magnet configurations for which the flux densities can be controlled as with an electromagnet.[2]

The static magnetic field from a single magnet depends on the shape of the magnet and offers minimal flexibility for configuration. Therefore, magnetic circuits containing multiple magnets and/or ferromagnetic components (e.g., flux guides, pole-pieces) are often utilized to configure a static magnetic field. However, the presence of strong magnetic force (e.g., $\sim 10^5$ N/m$^2$ for two magnets in direct contact) between magnets and/or ferromagnetic components leads to complicated fabrication methods for a given magnetic circuit. The majority of permanent magnet circuits is, therefore, fabricated manually requiring bonding materials, specialized equipment, and experience.

A prevalent approach to obtain a defined magnetic field is to use Halbach arrays. The Halbach array is an arrangement of multiple magnets placed in specific orientations.[3] Over the years, Halbach arrays have greatly influenced the use of permanent magnets for many applications.[4–10] However, a key factor that is often overlooked when considering a Halbach array is the difficulty in fabrication—multiple magnets in specific orientations requires specialized tools to assemble. Furthermore, unavoidable variations in magnetic moments of manufactured magnets can lead to complexity in obtaining reproducible designs.[11] Nevertheless, due to their unique ability to superposition magnetic fields from individual magnets, Halbach assemblies are frequently considered for obtaining desired magnetic field configurations. Figure 1(a) shows an ideal Halbach ring in which the polarization varies continuously along the circumference to obtain uniform field distribution inside the ring. In practice, however, it is difficult to implement such continuous distribution of polarization in "hard" magnetic materials, and therefore, discrete approximation of Halbach arrays are built from individual magnets polarized in desired directions.[4,5,11] An interesting observation can be made in the magnetic field distribution outside of a diametrically magnetized cylindrical magnet—the direction of

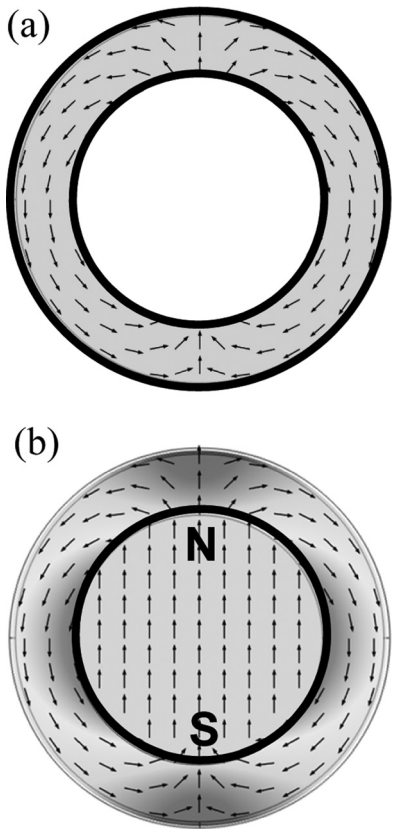


FIG. 1. (a) Schematic diagram of a continuously polarized (polarization direction shown by black arrows) ideal Halbach ring. (b) COMSOL simulation (arrow plot) from a diametrically magnetized cylinder. The arrows indicate the polarization of the magnetic field along the circumference of the cylinder.

[a)]P. Nath and C. K. Chandrana contributed equally to this work.
[b)]Author to whom correspondence should be addressed. Electronic mail: pulakn@lanl.gov



 

the magnetic field varies continuously along the circumference in a manner that mimics the distribution of an ideal Halbach ring (Figure 1(b)).

In this work, we present a magnet assembly that takes advantage of the special field distribution of a cylindrical magnet. The design consists of a diametrically magnetized ring-shaped, cylindrical permanent magnet placed inside a concentric ferromagnetic ring (Figure 2). The ferromagnetic ring gets magnetized according to the magnetic field distribution of the cylindrical ring magnet, i.e., magnetizing the ferromagnetic ring in a continuous polarization pattern similar to an ideal Halbach design. As a result, the magnetic field inside the air gap of the ring magnet produces the superposition of the field generated by the ring magnet and the magnetized ferromagnetic ring. The ring magnet is referred to as the "ring" and the ferromagnetic ring is referred to as the "shim" and hence, the name "Shim-a-ring" magnet.

To model a "Shim-a-ring" magnet, the design was categorized into four regions (Figure 2):

1. Ring region: A diametrically magnetized ring magnet (magnetization direction is indicated by arrows). The ring has an inner diameter of $ID_M$ and an outer diameter of $OD_M$.
2. Air gap region: An air gap inside the ring where the magnetic field is evaluated.
3. Shim region: A ferromagnetic ring, which is concentric to the ring region. The inner diameter and the outer diameter of the shim are represented by $ID_S$ and $OD_S$, respectively.
4. Spacing region: An annular gap between the shim and the ring. The width of the annular region is represented by $S_{MS}$.

The static magnetic field distributions of the model were calculated using the Finite Element Modeling (FEM) software COMSOL 4.3 (Burlington, MA) in 3D. Magnetostatic problems in COMSOL essentially solve the Possion's equation

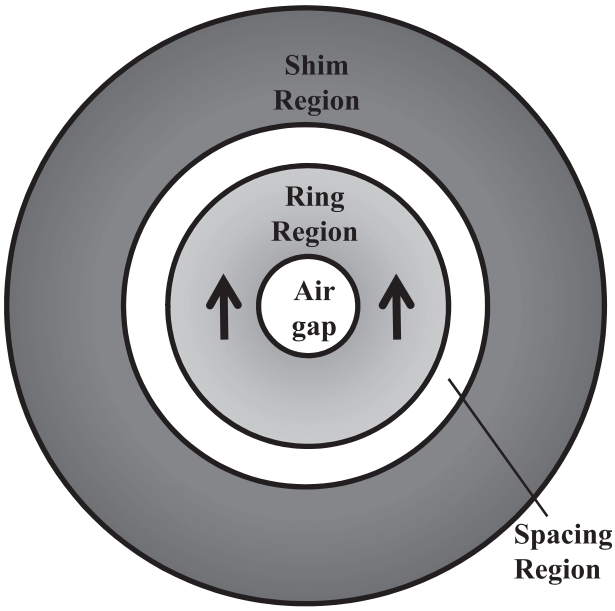


FIG. 2. Schematic diagram showing the different regions of a "Shim-a-ring" magnet design.

$$-\nabla \cdot (\mu_o \mu_r \nabla V_m - \mathbf{B_r}) = 0, \quad (1)$$

where $\mu_o$ is the permeability of free space, $\mu_r$ is the relative permeability of magnetically isotropic materials, $V_m$ is the scalar magnetic potential, and $\mathbf{B_r}$ is the remnant flux density. COMSOL allows the construction of a 3D model of the intended design using a graphic user interface. Magnetic insulation is assumed at the boundaries of the overall computational volume. To avoid the insulating boundary condition affecting the calculation, the size of the overall computational volume is kept large relative to the magnet model. A finite element mesh can be generated using a meshing tool. Mesh resolution in the volumes of interest are generally kept very high such that the results are not affected by the total number of elements. Different types of solvers are available to calculate the magnetic flux densities at any point of the model. The parameters used in our COMSOL model are presented in the supplementary materials.[12] Magnetic flux densities are analyzed inside the air gap region. Three different cross-sections of the air gap region were analyzed: (1) circular; (2) rectangular; and (3) triangular. The outer diameter of the magnet ($OD_M$), the inner diameter of the shim ($ID_M$), and the outer diameter of the shim ($OD_M$) were set to 40 mm, 40 mm, and 80 mm, respectively. This meant that there was no space between the magnet and the shim (i.e., $S_{MS} = 0$). The length of the magnet and shim ($t_z$) was set to 50 mm. Figure 3(a) shows the geometric parameters of the different cross-sections of the air gap analyzed by 3D finite element modeling. The origin (0,0) is located at the center of the concentric ring and the shim. Flux density distributions (Figure 3(b)) presented in this paper were analyzed between (−5,0) and (5,0) along the x-axis. The magnetization direction of the magnet was along the y-axis. For an air gap with circular cross-section, a uniform field distribution of 0.54 T was observed. Magnetic field distribution like this would be applicable to applications such as NMR, MRI, magnetic refrigeration, and charged particle manipulations. A square opening produced axisymmetric, gradually changing (6th order polynomial) gradient field distribution. This type of field distribution could be beneficial for magnetophoresis applications, where the gradual increase in the field could provide controlled spatial trajectories of magnetic particles with varying magnetic moments. The triangular opening generated mostly unidirectional, linearly changing gradient fields of ~85 T/m. The linear gradients are affected by the fringe fields close to the vertex of the triangle. Furthermore, we found that the design is suitable for obtaining a tunable field from a given magnet. Adjustable magnetic flux can be used for Electron Paramagnetic Resonance (EPR) applications.[4] Figure 4 shows the variable magnetic field obtained from a "Shim-a-ring" with circular shaped air gap ($ID_M = 10$ mm, $OD_M = 40$ mm). The magnetic flux increased with increasing the $OD_S$ at a fixed $ID_S = 40$ mm. Similarly, the magnetic flux decreased with increasing $ID_S$ at a fixed $OD_S = 80$ mm. Maximum flux density attainable with this configuration was around 0.54 T. However, a higher flux density can be obtained by using a higher grade NdFeB magnet and by using smaller diameter of the circular air gap. Nevertheless, finite element modeling showed a trend which indicates the flux densities attainable with the shim-a-ring

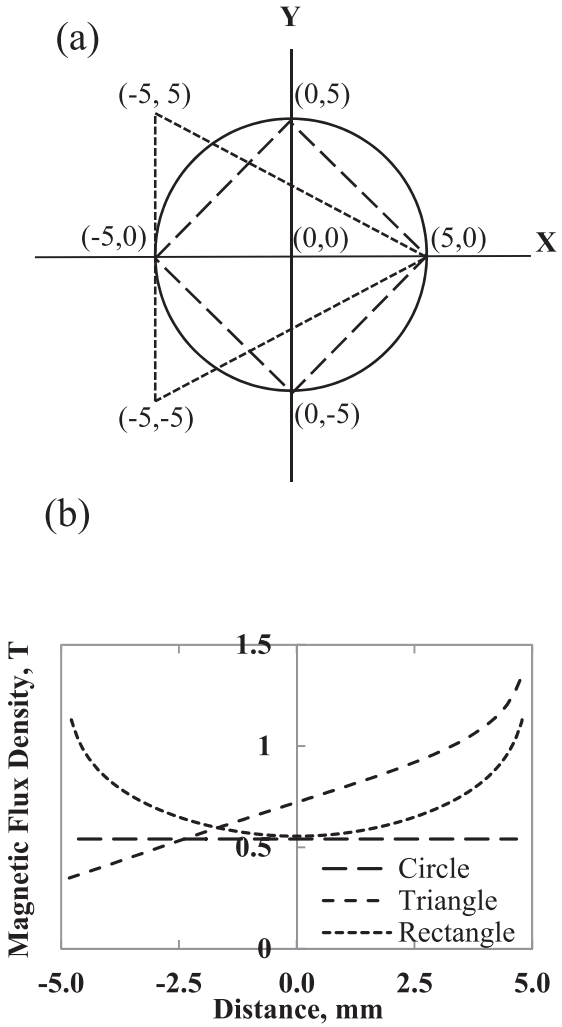


FIG. 3. (a) Geometric parameters of the different cross-section shape of the air gap; (b) Graphs showing magnetic flux densities along x-axis for different cross-section shapes of the air gap.

design would reach a maximum, which is dependent on the aspect ratio $ID_M/OD_M$ for a given $ID_S/OD_S$.

Different "Shim-a-ring" models were fabricated using N35 grade NdFeB ring shaped magnets (Storch Magnetics, Livonia, MI) with the dimension $ID_M = 10$ mm; $OD_M = 40$ mm; and $t_z = 50$ mm. The shims were fabricated in house with low carbon steel. One prototype of a "Shim-a-ring" magnet was assembled using a shim with $ID_S = 40$ mm and $OD_S = 80$ mm. The resulting magnetic field inside the air gap was then measured using a Tesla meter (Model 6010, FW Bell, Milwaukie, OR). The probe (STD 61-0205-05) was mounted on a x-y-z translation stage to measure the magnetic flux densities at precise locations of the air gap. Measured flux densities and the calculated flux densities for the magnet are presented in the supplemental materials[12]—validating the integrity of our modeling approach. To demonstrate the tunable aspect, a second model of a "Shim-a-ring" magnet was developed using a ring with a circular air gap (ID: 10 mm; OD: 40 mm) and multilayer low carbon steel shims (dimensions of the multilayer shims are presented in the supplemental materials[12]). In this design, the smallest shim was designed such that there is a concentric space ($S_{MS} = 4$ mm) between the magnet and the shim. This allowed the removal of individual layers of the shim without any mechanical tools. In this particular design, $S_{MS}$ was equal to 4.0 mm. Therefore, the spacing was fitted with acrylic rings, which had inner and outer diameters of 40 mm and 48 mm, respectively. Sequential addition of individual layers produced varying flux densities inside the air gap (Figure 5).

All fabrications of "Shim-a-ring" magnets were carried out via natural interaction between the ring magnet and the shim. The ring magnets were custom fabricated using CNC (computer numerical control) tools. The ring automatically assembles into the shim (a video showing the simplicity of fabrication is available as supporting online material[12]) and produced defined magnetic fields inside the air gap of the ring. "Shim-a-ring" magnets with different shape air gaps were fabricated. (Pictures and magnetic flux density measurements are presented in the supplementary materials.[12]) In the case where spacing is required between the shim and the ring, an acrylic ring was used to hold the magnet coaxially with the shim. Unlike a conventional Halbach ring, it is not necessary to manually align multiple magnets in specific orientations while working against the natural interaction of the magnets. Therefore, the design is suitable to automatically fabricate permanent magnet circuits without the need for any specialized equipment. This design is also scalable—especially for

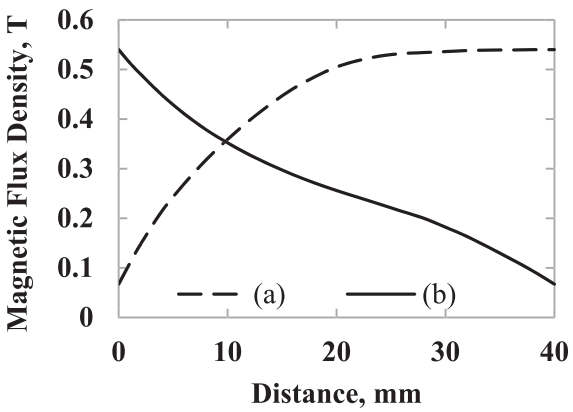


FIG. 4. Graphs showing the variable magnetic flux densities calculated at the center of a "Shim-a-ring" magnet with a circular air gap: (a) fixed $ID_S$ and varying $OD_S$; (b) fixed $OD_S$ and varying $ID_S$.

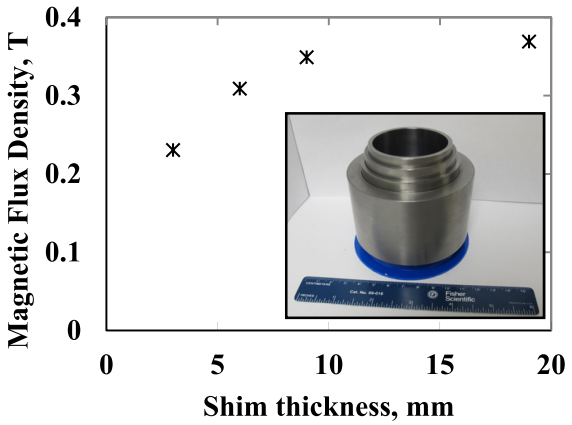


FIG. 5. Experimental measurement of variable magnetic fields with a multilayer shim for a "Shim-a-ring" magnet with circular air gap and $S_{MS} = 4.0$ mm (Inset: photograph of the multilayer shims).

miniaturization. Permanent magnets are being widely used for portable electronics and microfluidic applications.[13] Difficulties associated with creating Halbach arrays are compounded when producing miniaturized magnetic circuits based on multiple magnets for micro-scale applications. Miniaturization of "Shim-a-ring" designs would be simple and would only be limited by the machining ability of the ring magnet.

A design similar to the "Shim-a-ring" magnet has been discussed previously,[14] but only to produce "on/off" and variable fields by moving the shim across the axis of the magnet. However, we have observed that once the shim is placed, it is difficult to move it with respect to the ring without using specialized tools. The "Shim-a-ring" design takes advantage of the attraction between the shim and the magnet to obtain a stable magnetic circuit without the need for any bonding materials or mechanical means. With the exception of Halbach designs, there are not many magnetic assemblies that can produce tunable and configurable static magnetic fields. Due to the difficulties in fabricating Halbach magnets, wide-spread applications have been limited. The "Shim-a-ring" magnet's self-assembly nature simplifies fabrication of magnet assemblies even for workers unskilled with permanent magnet fabrication. The simplicity of fabrication and flexibility of designing different types of magnetic field distributions with the "Shim-a-ring" magnet provide the potential to replace traditional permanent magnet circuits for a broad range of applications that include NMR, MRI, magnetic refrigeration, magnetic separation, electrical motors, and charge particle manipulations.

This work was supported by Los Alamos National Laboratory's Laboratory Directed Research and Development (LDRD) program (Project No. 20110166ER).

[1]J. M. D. Coey, J. Magn. Magn. Mater. **248**(3), 441–456 (2002).
[2]R. Bjørk, C. R. H. Bahl, A. Smith, and N. Pryds, J. Magn. Magn. Mater. **322**(22), 3664–3671 (2010).
[3]K. Halbach, Nucl. Instrum. Methods **169**(1), 1–10 (1980).
[4]S. Anferova, V. Anferov, J. Arnold, E. Talnishnikh, M. A. Voda, K. Kupferschläger, P. Blümler, C. Clauser, and B. Blümich, Magn. Reson. Imaging **25**(4), 474–480 (2007).
[5]R. Bjørk, C. R. H. Bahl, A. Smith, D. V. Christensen, and N. Pryds, J. Magn. Magn. Mater. **322**(21), 3324–3328 (2010).
[6]E. Danieli, J. Mauler, J. Perlo, B. Blűmich, and F. Casanova, J. Magn. Reson. Imaging **198**(1), 80–87 (2009).
[7]Y. Yu, Y. Wang, and F. Sun, paper presented at 6th International Forum on Strategic Technology (IFOST), 2011.
[8]P. Cheiney, O. Carraz, D. Bartoszek-Bober, S. Faure, F. Vermersch, C. M. Fabre, G. L. Gattobigio, T. Lahaye, D. Guéry-Odelin, and R. Mathevet, Rev. Sci. Instrum. **82**(6), 063115 (2011).
[9]P. Babinec, A. Krafčík, M. Babincová, and J. Rosenecker, Med. Biol. Eng. Comput. **48**(8), 745–753 (2010).
[10]K. Atallah and D. Howe, IEEE Trans. Magn. **34**(4), 2060–2062 (1998).
[11]H. Raich and P. Blümler, Concepts Magn. Reson., Part B **23B**(1), 16–25 (2004).
[12]See supplementary material at http://dx.doi.org/10.1063/1.4807778 for (1) a video showing the fabrication of the "Shim-a-ring" magnet; (2) parameters used for COMSOL simulations; (3) Dimensions of the multilayer shim; (4) Graphs showing comparison of simulation and measurement data of a "Shim-a-ring" magnet with circular cross-section; (5) Characteristics of a "Shim-a-ring" magnet with square cross-section; (6) Characteristics of a "Shim-a-ring" magnet with triangular cross-section.
[13]N. Pamme, Lab Chip **6**(1), 24–38 (2006).
[14]P. Quanling, S. M. McMurry, and J. M. D. Coey, IEEE Trans. Magn. **39**(4), 1983–1989 (2003).